# Saturnian Trapped Radiation and Its Absorption by Satellites and Rings: The First Results from Pioneer 11

Abstract. *Electrons and protons accelerated and trapped in a Saturnian magnetic field have been found by the University of Chicago experiments on Pioneer 11 within 20 Saturn radii* ($R_S$) *of the planet. In the innermost regions, strong absorption effects due to satellites and ring material were observed, and from* $\sim 4$ $R_S$ *inwards to the outer edge of the A ring at 2.30* $R_S$ *(where the radiation is absorbed), the intensity distributions of protons* ($\geq 0.5$ *million electron volts) and electrons (2 to 20 million electron volts) were axially symmetric, consistent with a centered dipole aligned with the planetary rotation axis. The maximum fluxes observed for protons* ($> 35$ *million electron volts and for electrons* $> 3.4$ *million electron volts) were* $3 \times 10^4$ *and* $3 \times 10^6$ *per square centimeter per second, respectively. Absorption of radiation by Mimas provides a means of estimating the radial diffusion coefficient for charged particle transport. However, the rapid flux increases observed between absorption features raise new questions concerning the physics of charged particle transport and acceleration. An absorption feature near 2.5* $R_S$ *has led to the discovery of a previously unknown satellite with a diameter of* $\lesssim 200$ *kilometers, semimajor axis of 2.51* $R_S$, *and eccentricity of 0.013. Radiation absorption features that suggest a nonuniform distribution of matter around Saturn have also been found from 2.34 to 2.36* $R_S$, *near the position of the F ring discovered by the Pioneer imaging experiment. Beneath the A, B, and C rings we continued to observe a low flux of high-energy electrons. We conclude that the inner Saturn magnetosphere, because of its near-axial symmetry and the many discrete radiation absorption regions, offers a unique opportunity to study the acceleration and transport of charged particles in a planetary magnetic field.*

The Pioneer 11 encounter with Saturn on 1 September 1979 (*1*) provided the first opportunity to determine whether charged particles are accelerated and trapped in a Saturn magnetic field. This is the primary objective of our experimental investigation at Saturn, our purpose being to extend our knowledge of the physics of particle acceleration and loss in planetary magnetospheres beyond that gained from our studies at Earth, Jupiter (*2, 3*), and Mercury (*4*). Prior to this encounter, the only reasons for suggesting the presence of a magnetic field and trapped radiation at Saturn were first, the single set of observations of nonthermal radio bursts from the direction of Saturn made on the Earth satellite IMP-6 (*5*); and, second, the qualitative argument that Saturn might have an intrinsic magnetic field—since encounters with other planets having relatively high angular momenta have shown that they also have magnetospheres with stably trapped radiation. Various models for a Saturn magnetosphere have been suggested (*6, 7*).

In this report we describe our initial findings and conclusions derived from the University of Chicago experiment on Pioneer 11, which measures electrons, protons, and heavier nuclei over a wide range of energies and particle intensities. Although we have examined only the preliminary data and trajectory information, we do not expect that our results will change significantly when the final data and trajectory are taken into account. Dyer (*1*) has discussed details of the mission profile, spacecraft operation, and trajectory with respect to Saturn. Our instrument, described elsewhere (*3, 8*), includes four charged particle sensor systems (two especially designed for trapped radiation studies) to identify charged particle species and to measure particle intensities and spectra for kinetic energies $\gtrsim 1$ MeV. The instrument was functioning normally at encounter.

We present the data in terms of the distance from Saturn in Saturn radii, $R_S$ ($1\ R_S \equiv 60{,}000$ km), or in terms of the magnetic shell parameter $L \equiv R \cos^{-2}\lambda$, where $R$ is the distance from the center of the dipole in Saturn radii and $\lambda$ is the magnetic latitude. We have adopted a model of the Saturn magnetic field that is based on results from the magnetometer experiment (*9*). It consists of a dipole aligned with Saturn's rotation axis but offset $\sim 0.04\ R_S$ toward the north pole of the planet. Our analysis shows that an off-axis offset must be $< 0.01\ R_S$ to satisfy our charged particle observations. Since the Pioneer 11 trajectory was near-equatorial, $L \sim R$, except where otherwise noted.

*The outer magnetosphere.* Figure 1 shows the counting rates of protons with energies of 0.5 to 1.8 MeV, electrons with energies of 7 to 17 MeV, and the $> 3.4$ MeV electron flux (*10*) obtained over the period when Pioneer 11 was inside the Saturn magnetosphere. Outbound magnetopause and bow shock crossings occurred first at 30.3 and 49.3 $R_S$ (*11*), respectively, and are not shown in Fig. 1. Pioneer 11 entered the magnetosphere at a time when it was compressed by high-speed solar wind [$\sim 600$ km/sec (*11*)] and when the interplanetary fluxes of protons and electrons from known solar flares were factors $\sim 10^2$ to $10^3$ above interplanetary background levels. Consequently, in the data so far available we have not identified either any radiation in interplanetary space associated with Saturn, or any accelerated particles associated with bow shock crossings such as we observed at Jupiter (*12, 13*).

Inside $\sim 15\ R_S$, the intensity of 0.5 to 1.8 MeV protons as measured by the low-energy telescope (LET) began to increase inward as a result of trapping and acceleration of particles in Saturn's dipole field region. Outside 15 $R_S$, the spectrum, intensity, and proton to helium ratio measured by the LET were consistent with the interplanetary flux, $J$, resulting from solar flares. For a spectrum of the form $dJ/dE \propto E^{-\gamma}$, $\gamma$ in this region was found to be $2.0 \pm 0.3$, and the proton to helium ratio was $\sim 30$. Inside 15 $R_S$, the spectrum steepened to a value of $\gamma = 4.5 \pm 0.3$ over the region 13 to 5 $R_S$, and the proton to helium ratio increased to $\sim 500$, establishing that the dominant nucleonic component of Saturn's trapped radiation consists of protons.

A large intensity decrease for low-energy protons took place between 7 and 4 $R_S$. Evidence of absorption of particles by Dione and Enceladus is present, but satellite absorption alone does not appear to account for the overall intensity decrease. Although the flux of low-energy ($\sim 7$ to 17 MeV) electrons was considerably above background and interplanetary levels in the region where the large proton intensity decrease was observed, the electron intensity did not show any decrease corresponding to that for the protons. The rate of rise toward lower $L$ did, however, decrease. A proper interpretation of this proton intensity decrease must account for the differing behavior of electrons and protons. The existence of an E ring (*14*) provides a possible explanation for this decrease through absorption by ring material. In this case, as pointed out by Thomsen and Van Allen (*15*), the relative effectiveness of absorption for electrons and protons may be used to infer the size of ring particles. Alternatively, since evidence for a hot plasma has been found in this region (*11*), the proton intensity decrease may result from scattering by wave-particle interactions so that trapped protons are lost to the atmosphere at high latitudes.


0036-8075/80/0125-0411$01.00/0 

The main differences in intensity inbound and outbound for $R > 4\ R_S$ may arise from either time-dependent compressions of the magnetosphere or the appearance of tail-like current sheets outbound (9), or both.

*The inner magnetosphere.* To demonstrate the remarkable axial symmetry and stability inside 4 $R_S$, we have overlaid the inbound and outbound counting rates of the protons from Fig. 1A to show in Fig. 2 the nearly identical intensity profiles inbound and outbound. This symmetry reflects the alignment of the dipole magnetic moment with the axis of planetary rotation. Similar plots reveal essentially the same symmetry for other measured fluxes. The largest difference found was a factor ~ 3 for the peak values of the intensities inbound and outbound within $L \sim 2.8$ for electrons > 3.4 MeV (Fig. 1B). Protons with energies > 35 MeV, which were measured by the fission cell detector (3, 8), reach maximum flux levels of $3 \times 10^4$ protons $cm^{-2}\ sec^{-1}$ inside $L = 4$.

*Radiation absorption by Mimas.* A clear example of trapped radiation absorption by a satellite of Saturn is that observed at the orbit of Mimas. We show in Fig. 3 an expanded view of the trapped radiation intensity profile near the orbit of Mimas inbound. The outbound profile is essentially identical. The study of this absorption phenomenon is important since it provides a means for determining the parameters describing the inward diffusive motions which we believe to be responsible for the maintenance and acceleration of the trapped radiation. The method of analysis is similar to that carried out at Jupiter using particle absorption by the satellite Io (3). For the proton flux in Fig. 3 (and also on the outbound pass) the width of the flux minimum corresponds almost exactly to the radial range swept out by Mimas as a result of the eccentricity of its orbit. This suggests that the offset of the dipole moment in the equatorial plane is small, since a significant offset would tend to increase the radial range over which absorption effects are observed. The nearly constant counting rate observed in this minimum suggests a residence time for particles in the region much longer than the orbital period of Mimas (22.56 hours). These observations set an upper limit on the inward diffusion coefficient, $D$, at the orbit of Mimas. Since the particles must survive for a period $T > 23$ hours, and since Mimas's known eccentricity ($\epsilon = 0.02$) yields a $\Delta L$ for possible absorption of 0.12, we find from the relation $D \sim (\Delta L)^2/4T$ that $D < 4 \times 10^{-8}\ R_S^2$/sec. In fact, consideration of the orbital motion of Mimas relative to the drift and latitudinal bounce motions of the trapped particles leads to a mean survival time which is substantially longer than the Mimas orbital period, so that, most probably, $D < 10^{-8}\ R_S^2$/sec, at $L = 3.1$.

Table 1. Satellite parameters.

| Satellite | Radius (km) | Semimajor axis ($R_S$) | Eccentricity |
|---|---|---|---|
| 1979 S 2 | > 100 | 2.51 | 0.013 |
| Janus | ~ 110* | 2.65*, 2.81* | 0* |
| Mimas | ~ 170* | 3.09* | 0.02* |

*Earth-based observations.

Figure 3 reveals that absorption appears more effective for protons than for the high-energy electrons, possibly implying a significantly different diffusion coefficient for the two particle species. Also apparent in Fig. 3 is a sharp intensity decrease observed inbound only, lasting approximately 1 minute, which is observed for both protons and electrons near ~ 1420 UT. This cannot be a direct "shadow" of Mimas since Mimas has passed the point where Pioneer 11 crossed its orbit ~ 3 hours prior to the arrival of the spacecraft.

*Janus.* Since we find no effect in our data that can be attributed to an absorption by Janus at 2.65 $R_S$ (Fig. 4), we suggest that the intensity plateau observed at ~ 2.8 $R_S$ (1435 UT, Fig. 3) may result from absorption of trapped radiation by Janus if the orbital radius of Janus is 2.81 $R_S$, as determined by Franklin *et al.* (16), rather than 2.65 $R_S$, as determined by Dollfus (17) and, more recently, by Fountain and Larson (18).

*Evidence for a new satellite.* We have found near $L = 2.5$, inbound and outbound, an absorption-like feature (Fig. 4) which is very similar to that observed for Mimas—including a relatively constant intensity interval at $2.49 \leq L \leq 2.55$. This feature also was seen for protons > 35 MeV as measured by the fission cell detector. Outbound, the absorption effect was observed soon after the spacecraft finished transmitting data stored during occultation. Furthermore, during encounter operations, Rairden noted [see (19)], and Fillius *et al.* (20) and ourselves confirmed, that there was an unexplained intensity drop for 10 to 12 seconds at ~ 2.5 $R_S$ inbound. We then went on to note and report (21) that this disappearance of flux (shown in Fig. 4A) was probably the result of the passage of the spacecraft through the magnetic flux

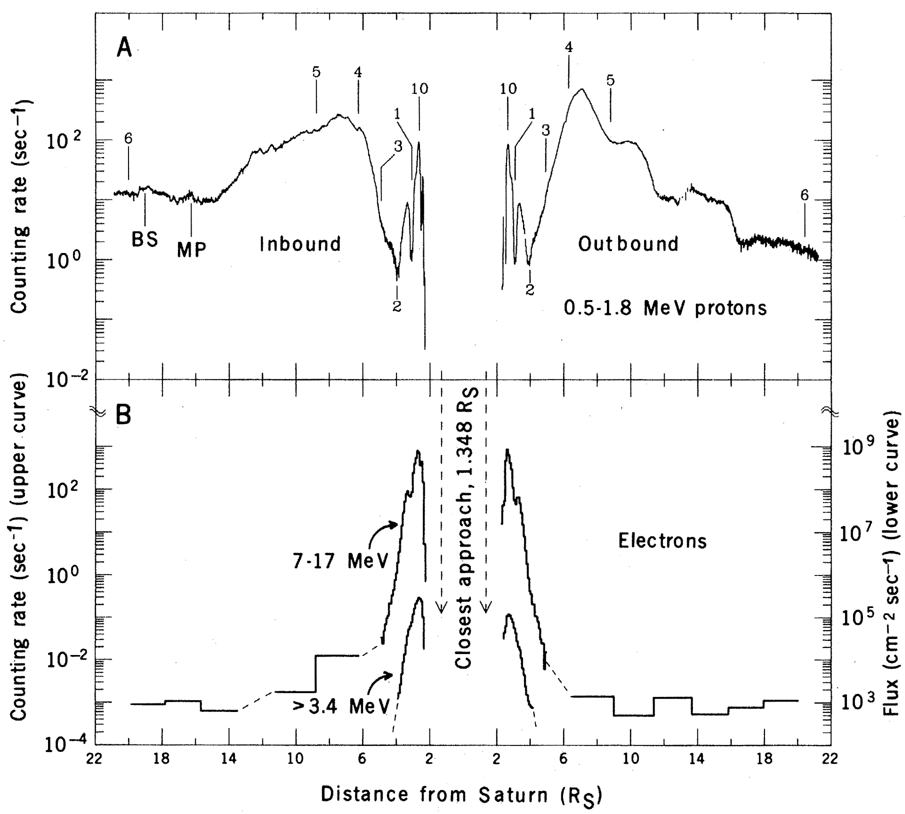


Fig. 1. (A) Proton intensity measured by the LET (8). Interplanetary background level is ~ $2 \times 10^{-2}$ count/sec. Saturn satellite locations (26): 1, Mimas; 2, Enceladus; 3, Tethys; 4, Dione; 5, Rhea; 6, Titan; and 10, Janus. *BS*, bow shock crossing; *MP*, magnetopause crossing. (B) Electron intensities: > 3.4 MeV energies measured by the electron current detector (ECD); 7- to 17-MeV energies measured by the main telescope (3, 8). The 7- to 17-MeV electron intensity is a nonlinear function of the counting rate inside $L \sim 5$.

tube of a previously unknown satellite of Saturn. We reported at that time that the radial extent of the flux disappearance was 170 to 200 km, which gives a lower limit for the satellite's diameter.

During the period when the electron counting rate was near zero (Fig. 4A) our instrument was still analyzing protons in the energy range ~ 10 to 20 MeV. This leads to two important conclusions: (i) the instrument was functioning normally and (ii) since the 10-MeV proton gyroradius was ~ 300 km and the 3-MeV electron gyroradius was ~ 10 km, the large change in proton to electron ratio implies that the scale size of the object must be of the order of 100 km, consistent with estimates obtained from the duration of the event.

Because the opposite directions of the azimuthal drift motions of electrons (westward) and protons (eastward) in the magnetic field would separate their initial flux tube positions at the relative rate of ~ 30 km/sec, and since we observe the decreases in proton and electron intensity to be coincident to within ~ 3 seconds, we infer that the spacecraft must have passed almost directly under the suspected satellite. On other trajectories a sharp decrease in only the proton or only the electron flux would have been observed. Any such satellite is probably in, or very near, the equatorial plane which then places it ~ 2500 km above the spacecraft at the time of the disappearance of flux in Fig. 4. As noted by Anderson *et al.* (*22*), at this distance the absence of perturbations in the trajectory due to the mass of the object places an upper limit on the radius of about 100 km for an assumed density of 1.5 g/cm$^3$. A narrow ring of matter could not account for our observations since no absorption feature corresponding to such a ring was observed on the outbound pass.

If, as at Mimas, we equate the radial width of the overall absorption profile (0.064 $R_S$) to the radial excursion of the new satellite in its orbit, and the center of the absorption ($L$ = 2.51) to the semimajor axis of the orbit, we obtain an eccentricity of $\epsilon$ = 0.013. As we note later, the radial range of this absorption cannot be accounted for by an offset dipole. Our estimates for the various characteristics of this satellite are summarized in Table 1. It is likely that this is the same satellite whose existence was suggested by Fountain and Larson (*18*) and may also be the new satellite observed by the Pioneer imaging experiment (*23*). However, considering the large reported uncertainties in the orbital parameters for Janus, we cannot yet exclude the possibility that the satellite we have identified is Janus.

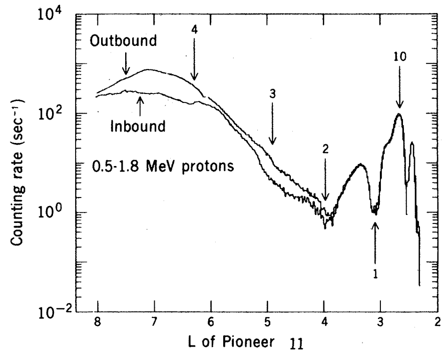


Fig. 2. Inbound and outbound proton intensities from Fig. 1A plotted against the magnetospheric trapping parameter $L$ ($\approx R$), which organizes the observations to show axial symmetry.

*Radiation absorption by ring material.* In Fig. 5 we show the absorption effect on 0.5- to 1.8-MeV protons and 7- to 17-MeV electrons due to material in the region $L$ = 2.34 to 2.36 $R_S$, which corresponds to the position of the F ring discovered by the Pioneer 11 imaging experiment (*23*). For the magnetic field model adopted, $L$ and the radius of the spacecraft, $R$, differ only by $\leq$ 0.006 $R_S$ throughout the interval shown in Fig. 5.

The radial range of the F ring, as shown in Fig. 5 between $L$ = 2.337 and $L$ = 2.360, corresponding to ~ 1100 km, was chosen to include the prominent, variable absorption features visible in the electron counting rates. That these variable and rapid decreases of intensity are not readily apparent in the lower proton counting rate is due, at least in part, to greater statistical uncertainty. The observed variable absorption of the electrons is probably the result of a nonuniform radial distribution of matter in the F ring. Furthermore, since three major intensity minima are observed inbound, but only two of these are reproduced in the outbound data, it is probable that the matter distribution in the F ring is not azimuthally uniform and may include one or more concentrations of matter.

The width of the absorption feature associated with the F ring allows us to place an upper limit on the equatorial offset of the center of Saturn's magnetic dipole. If the dipole were offset from the rotation axis of the planet by a distance $r$, then, in each half rotation of the planet, the F ring would absorb trapped radiation over a radial range $2r + w$, where $w$ is the width of the ring. The ~ 1100-km width of the absorption feature associated with the F ring places an upper limit on the equatorial offset of the magnetic dipole, neglecting the width of the ring, of $r < 0.01$ $R_S$. We find that all of our observations are consistent with this upper limit for the equatorial dipole offset, and thus are consistent with the analysis of the magnetic field reported by the magnetometer experiment group (*9*).

The range shown for the outer edge of the A ring in Fig. 5 ($L$ = 2.293 ± 0.017)

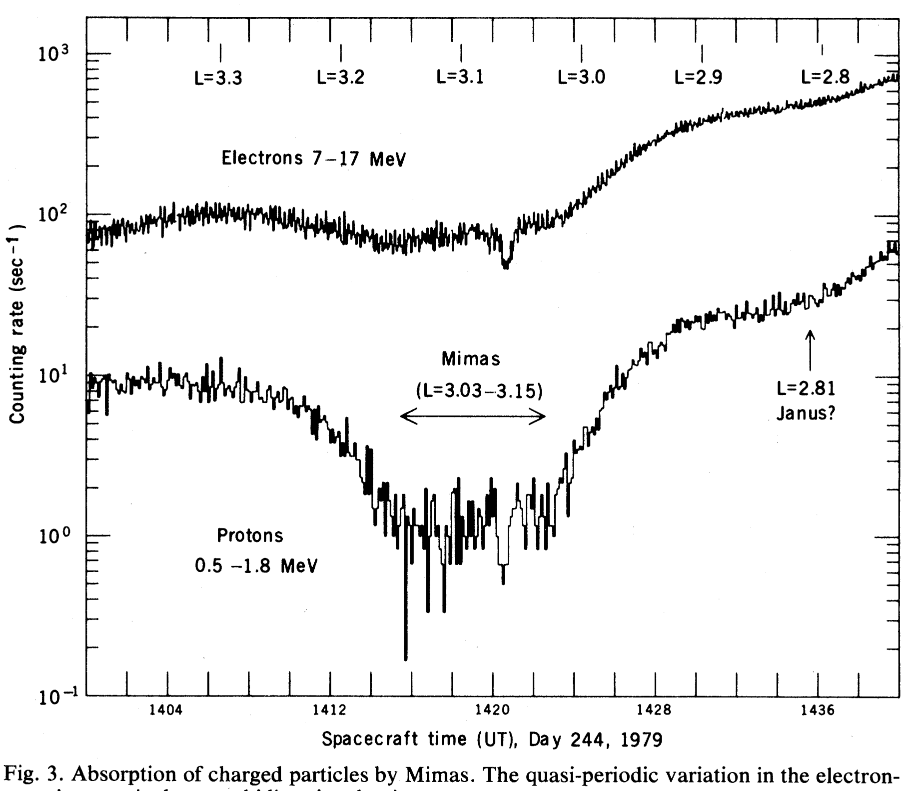


Fig. 3. Absorption of charged particles by Mimas. The quasi-periodic variation in the electron-counting rate is due to a bidirectional anisotropy.

Table 2. Maximum observed trapped radiation flux.

| Planet | Protons ($E \gtrsim 35$ MeV) | | Electrons ($E \gtrsim 3.4$ MeV) | |
|---|---|---|---|---|
| | Flux* | $L$ | Flux* | $L$ |
| Earth (*2, 3*) | $2 \times 10^4$ | 1.5 | $\sim 10^4$ | 1.5, 4 |
| Saturn | $3 \times 10^4$ | 2.7 | $3 \times 10^6$ | 2.5 |
| Jupiter (*3, 10*) | $10^7$ | 1.9 | $7 \times 10^7$ | 3.1 |

*Flux expressed as per square centimeter per second.

corresponds to the equatorial radius and uncertainty quoted by Pollack (*24*) from terrestrial observations. The apparent difference in proton and electron counting rate cutoffs appears to be due to the fact that the electron counting rate was $\sim 100$ times greater than the proton counting rate. Hence, the difference may be purely statistical. On the basis of our analysis of charged particle data and the preliminary spacecraft trajectory and magnetic field data, we conclude that the outer edge of the A ring is at a radial distance of $2.300 \pm 0.005$ $R_S$.

Between the F ring and the A ring [a region called the Pioneer division (*23*)] on the inbound pass, electron and proton counting rates reach maxima at $L = 2.32$ to 2.33. The rate of intensity increase for protons and electrons inward toward the maximum within the Pioneer division (as well as immediately inside the orbits of Mimas and the new satellite) seems to exceed predictions for acceleration by steady-state inward diffusion. Indeed, the flux increase toward decreasing $L$ appears to be so rapid in these regions that the density of particles in phase-space, whose radial gradient "drives" the diffusive flux (*25*), appears to increase inward rather than outward. If so, the charged particles should be transported outward rather than inward, and we are left with the question of how the interior region of the magnetosphere is populated with energetic particles if we are observing steady-state conditions. This question is under investigation.

*Under the A, B, and C rings*. The absorption of low-energy protons and electrons inside the outer edge of the A ring is so complete that the low-energy detector counting rates were comparable to laboratory conditions—by far the lowest level found anywhere during the mission. However, beneath the rings we find a residual flux of electrons in the energy range $\sim 2$ to 25 MeV with an extremely flat spectrum ($\propto E^{-0.6}$) and with an intensity that is about four to five times the interplanetary quiet-time electron flux. Because the Saturn magnetic rigidity cutoff for galactic cosmic rays in this re-

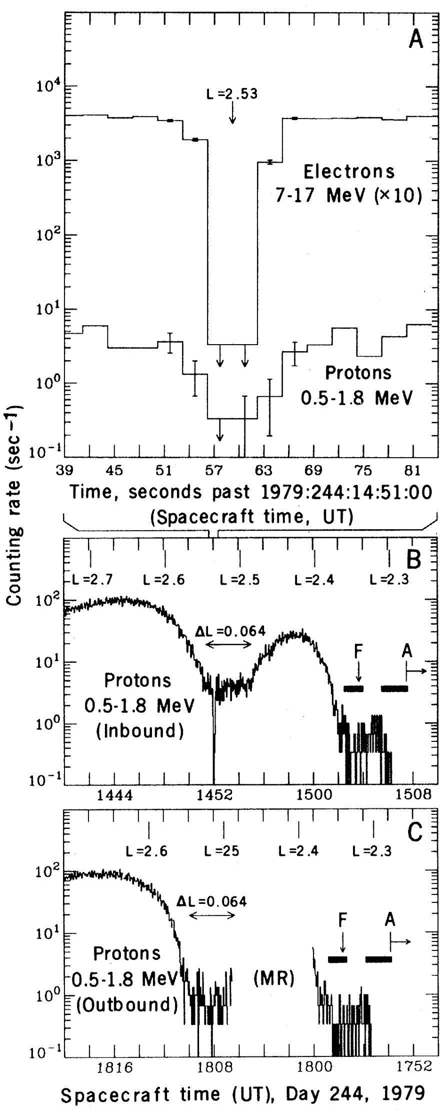


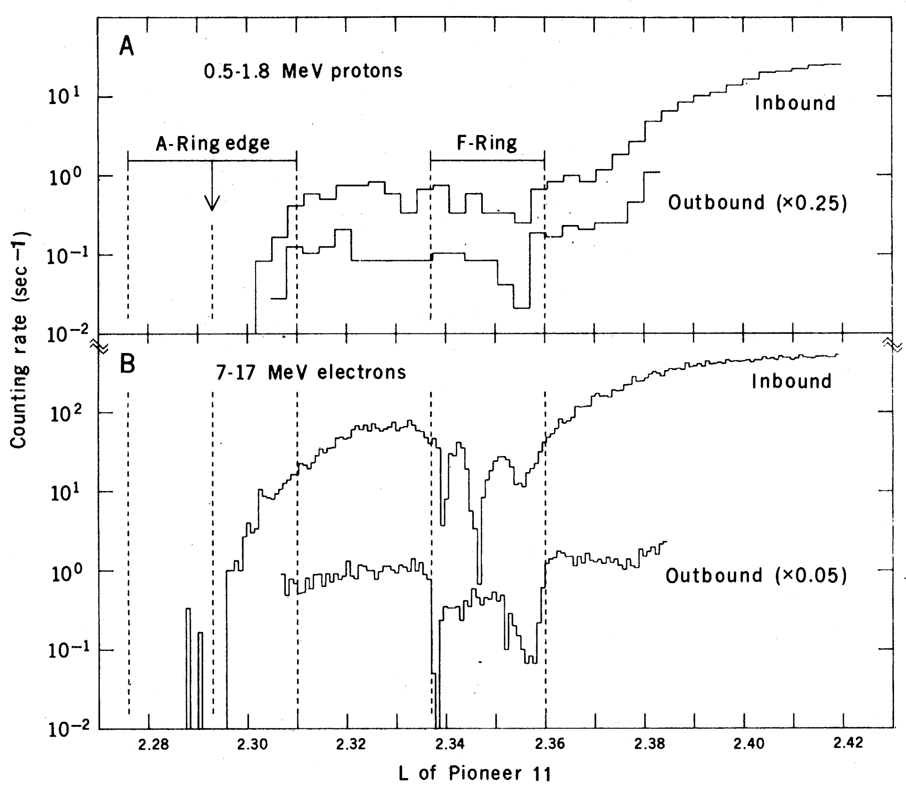


Fig. 4 (left). (A) Charged particle absorption during passage through the magnetic flux tube of a previously unknown satellite. Counting rates are 3-second averages with $1\sigma$ errors shown. (B) Absorption of trapped protons by the new satellite and by rings. The orbital eccentricity is determined from the radial range of the minimum intensity. *F* indicates the region of absorption by the F ring discovered by Pioneer 11; *A* indicates the outer edge of the A ring. The bars correspond to the dashed lines shown in Fig. 5. (C) Outbound profile of the charged particle absorption. The data gap (*MR*) is a result of the readout of data stored during occultation. The scatter in the counting rates is consistent with being purely statistical. Fig. 5 (right). The absorption effects of the A ring and the F ring on the energetic particle fluxes. (A) Twelve-second averages of the 0.5- to 1.8-MeV proton counting rates and (B) 3-second averages of the 7- to 17-MeV electron counting rate, with outbound data offset vertically below the inbound. The prominent absorption features visible in the electron counting rate associated with the F ring are indicated. The position of the outer edge of the A ring reflects a 1000-km uncertainty and is derived from terrestrial observations (*24*).

gion exceeds 12 GV from all directions of incidence, we conclude tentatively that these electrons are either the product of pion decay from cosmic-ray interactions with ring material, or the atmosphere of Saturn, or—more likely—trapped electrons that were first accelerated beyond the radius of the A ring and, subsequently, have been scattered in the magnetic field at high latitudes into $L \leq 2.3$.

*Conclusions*. We have discovered that, as at Earth and Jupiter, the magnetosphere of Saturn contains high-energy trapped nucleons and electrons and, as at Jupiter, radiation is absorbed by planetary satellites. Peak intensities of electrons and protons in these magnetospheres are shown in Table 2, and it is clear that the maximum trapped radiation intensities observed for Saturn lie between those of Earth and Jupiter. For the Pioneer 11 trajectory the fluence of $> 3.4$ MeV electrons was $9.1 \times 10^9$ cm$^{-2}$ [corresponding to 290 radiation units (silicon)].

Our data contain evidence for a new satellite of Saturn with a semimajor axis of 2.51 $R_S$—the first satellite to be discovered from analysis of energetic charged particle radiation. There also are absorption features, for example, at the orbit of Mimas and at the F ring, which may be accounted for by unknown satellites or clumps of ring material. The width and inbound-outbound symmetry of the observed absorption features are consistent with a spin-aligned dipole magnetic moment offset from the rotation axis by no more than 0.01 $R_S$. In some cases the radiation intensity profile appears to be inconsistent with predictions of a steady-state inward diffusion model for populating the inner-trapped radiation zones.

We conclude that the inner Saturn magnetosphere, because of its near-axial symmetry and the many discrete radiation absorption regions, offers a unique opportunity to study the acceleration and transport of charged particles in a planetary magnetic field. These and other questions, such as the strong and changing particle anisotropies that we have observed but have not discussed herein, will be discussed elsewhere.

J. A. SIMPSON
T. S. BASTIAN
D. L. CHENETTE
G. A. LENTZ
R. B. MCKIBBEN
K. R. PYLE
A. J. TUZZOLINO

*Enrico Fermi Institute,
University of Chicago,
Chicago, Illinois 60637*

**References and Notes**

1. J. W. Dyer, *Science* **207**, 400 (1980).
2. J. A. Simpson and R. B. McKibben, in *Jupiter*, T. Gehrels, Ed. (Univ. of Arizona Press, Tucson, 1976), pp. 738–766.
3. J. A. Simpson *et al.*, *J. Geophys. Res.* **79**, 3522 (1974).
4. J. A. Simpson, J. H. Eraker, J. E. Lamport, P. H. Walpole, *Science* **185**, 160 (1974).
5. L. W. Brown, *Astrophys. J.* **198**, L89 (1975).
6. C. F. Kennel, *Space Sci. Rev.* **14**, 511 (1973).
7. G. Siscoe, in *Solar System Plasma Physics*, C. Kennel, L. J. Lanzerotti, E. N. Parker, Eds. (North-Holland, Amsterdam, 1979), p. 319.
8. J. A. Simpson, G. A. Lentz, R. B. McKibben, J. J. O'Gallagher, W. Schroeder, A. J. Tuzzolino, *NSSDC Tech. Ref. File B21970* (Goddard Space Flight Center, Greenbelt, Md., 1974).
9. E. J. Smith, L. Davis, Jr., D. E. Jones, P. J. Coleman, Jr., D. S. Colburn, P. Dyal, C. P. Sonnett, *Science* **207**, 407 (1980).
10. Electrons > 3.4 MeV are measured by the ECD (*3*) with a calibration revised since the Pioneer 10 and 11 Jupiter encounters (*3*).
11. J. H. Wolfe, J. D. Mihalov, H. R. Collard, D. D. McKibbin, L. A. Frank, D. S. Intriligator, *Science* **207**, 411 (1980).
12. J. A. Simpson, D. Hamilton, G. Lentz, R. B. McKibben, A. Mogro-Campero, M. Perkins, K. R. Pyle, A. J. Tuzzolino, J. J. O'Gallagher, *ibid.* **183**, 306 (1974).
13. J. A. Simpson, D. C. Hamilton, G. A. Lentz, R. B. McKibben, M. Perkins, K. R. Pyle, A. J. Tuzzolino, J. J. O'Gallagher, *ibid.* **188**, 455 (1975).
14. W. A. Feibelman, *Nature (London)* **214**, 793 (1967).
15. M. F. Thomsen and J. A. Van Allen, *Geophys. Res. Lett.* **6**, 893 (1979).
16. F. A. Franklin, G. Colombo, A. F. Cook, *Icarus* **15**, 80 (1971).
17. A. Dollfus, *Astronomie* **6**, 253 (1968).
18. J. W. Fountain and S. M. Larson, *Science* **197**, 915 (1977).
19. J. A. Van Allen, M. F. Thomsen, B. A. Randall, R. L. Rairden, C. L. Grosskreutz, *Science* **207**, 415 (1980).
20. W. Fillius, W. H. Ip, C. E. McIlwain, *ibid.*, p. 425.
21. J. A. Simpson, news conference, 4 September 1979; *Trans. Am. Geophys. U.* **60**, 865 (1979).
22. J. A. Anderson, G. W. Null, E. D. Biller, S. K. Wong, W. B. Hubbard, J. J. MacFarlane, *Science* **207**, 449 (1980).
23. T. Gehrels *et al.*, *Science* **207**, 434 (1980).
24. James B. Pollack, *Space Sci. Rev.* **18**, 3 (1975).
25. W. N. Hess, *The Radiation Belt and Magnetosphere* (Blaisdell, Waltham, Mass., 1968).
26. D. Morrison, D. P. Cruikshank, J. A. Burns, in *Planetary Satellites*, J. A. Burns, Ed. (Univ. of Arizona Press, Tucson, 1977), pp. 3–17.
27. We are grateful to the Pioneer Project Office, especially to C. F. Hall, R. Hogan, and J. Dyer, and to the staff of the Laboratory for Astrophysics and Space Research of the Enrico Fermi Institute, particularly M. Perkins, R. Jacquet, and J. Lamport for their contributions to the instrumentation. We appreciate the assistance and advice of J. J. O'Gallagher, S. P. Christon, J. H. Eraker, S. Tejero, J. Cooper, and P. Kruley during the Saturn encounter and during the preparation of this report. We thank J. H. Wolfe and E. J. Smith for making available to us their preliminary plasma and magnetic field data, respectively. This work was supported in part by NASA/Ames NAS 2-6551 contract, NASA grant NGL 14-001-006, and NSF grant ATM 77-24494.

3 December 1979

## Saturn's Magnetosphere, Rings, and Inner Satellites

Abstract. *Our 31 August to 5 September 1979 observations together with those of the other Pioneer 11 investigators provide the first credible discovery of the magnetosphere of Saturn and many detailed characteristics thereof. In physical dimensions and energetic charged particle population, Saturn's magnetosphere is intermediate between those of Earth and Jupiter. In terms of planetary radii, the scale of Saturn's magnetosphere more nearly resembles that of Earth and there is much less inflation by entrapped plasma than in the case at Jupiter. The orbit of Titan lies in the outer fringes of the magnetosphere. Particle angular distributions on the inbound leg of the trajectory (sunward side) have a complex pattern but are everywhere consistent with a dipolar magnetic field approximately perpendicular to the planet's equator. On the outbound leg (dawnside) there are marked departures from this situation outside of 7 Saturn radii* ($R_S$)*, suggesting an equatorial current sheet having both longitudinal and radial components. The particulate rings and inner satellites have a profound effect on the distribution of energetic particles. We find (i) clear absorption signatures of Dione and Mimas; (ii) a broad absorption region encompassing the orbital radii of Tethys and Enceladus but probably attributable, at least in part, to plasma physical effects; (iii) no evidence for Janus (1966 S 1) (S 10) at or near 2.66* $R_S$*; (iv) a satellite of diameter* $\gtrsim$ *170 kilometers at 2.534* $R_S$ *(1979 S 2), probably the same object as that detected optically by Pioneer 11 (1979 S 1) and previously by ground-based telescopes (1966 S 2) (S 11); (v) a satellite of comparable diameter at 2.343* $R_S$ *(1979 S 5); (vi) confirmation of the F ring between 2.336 and 2.371* $R_S$*; (vii) confirmation of the Pioneer division between 2.292 and 2.336* $R_S$*; (viii) a suspected satellite at 2.82* $R_S$ *(1979 S 3); (ix) no clear evidence for the E ring though its influence may be obscured by stronger effects; and (x) the outer radius of the A ring at 2.292* $R_S$*. Inside of 2.292* $R_S$ *there is a virtually total absence of magnetospheric particles and a marked reduction in cosmic-ray intensity. All distances are in units of the adopted equatorial radius of Saturn, 60,000 kilometers.*

We report herein the discovery of the magnetosphere of Saturn and a survey of its characteristics. In addition, new findings on the rings and inner satellites of the planet are provided by the measurements of energetic charged particle distributions within the inner magnetosphere. Before Pioneer 11's flyby encounter with Saturn (periapsis on 1 September 1979) (*1*) there was only meager observational evidence on the basic question of whether or not this planet is magnetized (*2, 3*).

The University of Iowa instrument on


0036-8075/80/0125-0415$01.25/0 